





## ORIGINAL RESEARCH ARTICLE

## Analytical Investigation of Arrhenius Kinetics with Heat Source/Sink Impacts along a Heated Superhydrophobic Microchannel

Godwin Ojemer<sup>1\*</sup>, Isaac Obiajulu Onwubuya<sup>2</sup>, Emmanuel Omokhuale<sup>3</sup>,  
Abdullahi Hussaini<sup>4</sup> and Abdulsalam Shuaibu<sup>5</sup>

<sup>1,5</sup>Department of Mathematics, College of Sciences, Federal University of Agriculture, P. M. B. 28, Zuru, Kebbi State, Nigeria.

<sup>2</sup>Department of Mathematics, Faculty of Sciences, Air Force Institute of Technology, P. M. B. 2104, Kaduna State, Nigeria.

<sup>3</sup>Department of Mathematics, Faculty of Sciences, Federal University Gusau, P. M. B. 1001, Zamfara State, Nigeria.

<sup>4</sup>Department of Mathematics, Sokoto State University, P. M. B. 2134, Sokoto State, Nigeria.

### ABSTRACT

Exothermic Arrhenius-controlled chemical reactions are widely employed for heating applications, such as combustion in heating systems and fuel-burning motors. These effects are critical for manufacturing high thermal systems required for high thermal performances. Therefore, this paper presents the analytical investigation into the Arrhenius-controlled heat-generating/absorbing fluid of a hydromagnetic flow along a heated upstanding plate in a microchannel. One wall had a superhydrophobic surface and temperature jump conditions, but the other was unaltered. The regular perturbation approach investigated the nonlinear, coupled governing equations. With the help of graphical plots, the impacts of crucial and relevant parameters embedded in the flow are described. This investigation concludes that chemically reacting parameters' impact significantly elevates the micro-channel's thermal and hydromagnetic flow. However, applying the heat generation parameter increases fluid velocity, whereas the heat absorption parameter produces the contrary effect. The outcomes of this study can be relevant to the field of biomedical sciences and devices for improving heat transfer efficiency, chemical synthesis, enhancing the performances of micro-electromechanical systems (MEMS) and mini-devices, heating and energy generation, designing efficient energy conversion processes, and so on.

### ARTICLE HISTORY

Received September 01, 2023.

Accepted December 18, 2023.

Published February 17, 2024.

### KEYWORDS

Free convection, Arrhenius kinetics, superhydrophobic slip, heat generation/absorption, slit micro-channel



© The authors. This is an Open Access article distributed under the terms of the Creative Commons Attribution 4.0 License (<http://creativecommons.org/licenses/by/4.0>)

### INTRODUCTION

The swift advancement of science and technology in the wake of the demand for more compact and less heavy devices encourages the focus of the scientific group, engineers, and innovators on mini-technology, micro-technology, and eventually nano-technology. These innovations prompted computational fluid dynamics experts to shift the emphasis from analysing flows in macro-channels to studying flows in mini-channels, micro-channels, and nano-channels. Microfluidics have evolved immensely over the past decade due to their importance in material manufacturing, micro-energy pipes, space technology, micro-jet boundary layer cooling, high-performance computing, heavy power density transistors, and other devices. Because most of these simulations contain internal micro-channel transport, a sound knowledge of the flow features has become critical for correct flow projections and conceptualization (Jha and Gwandu 2017, Jha *et al.* 2014a). Several articles on the

influence of flow regimes on microstructure in various physical configurations have been published.

Regarding the aforementioned, Hamza *et al.* (2023a) recently used the homotopy perturbation technique to explore the implications of the hydromagnetic flow of a chemically reactive fluid in a microchannel. Later, Hamza *et al.* (2023b) conducted a theoretical analysis of Arrhenius-controlled heat transfer propagation in a microchannel caused by an imposed magnetic field. Ahmed *et al.* (2023) investigated the impact of thermal-hydraulic performance using high-fidelity conjugate heat transfer simulations to model a micro-channel heat exchanger. The study considers circular, triangular, and square micro-channel geometries with louver-shaped fins and provides insights into the effects of these geometries on heat transfer performance. Ojemer and Hamza (2022) used the homotopy perturbation technique to conduct a

**Correspondence:** Godwin Ojemer. Department of Mathematics, College of Sciences, Federal University of Agriculture, P. M. B. 28, Zuru, Kebbi State, Nigeria. ✉ [godwinojemer@gmail.com](mailto:godwinojemer@gmail.com). Phone Number: +234 806 167 6148.

**How to cite:** Ojemer, G., Obiajulu, I. O., Omokhuale, E., Hussaini, A., & Shuaibu, A. (2024). Analytical Investigation of Arrhenius Kinetics with Heat Source/Sink Impacts along a Heated Superhydrophobic Microchannel. *UMYU Scientifica*, 3(1), 37 – 47. <https://doi.org/10.56919/usci.2431.004>

steady, fully developed analysis of an Arrhenius kinetically propelled heat-generating or absorbing fluid in a microchannel. [Jha and Malgwi \(2019a\)](#) described the consequences of Hall and ion slip influence on the flow of MHD heat in an upward micro-channel instigated by an applied magnetic field. As part of their work, [Jha et al. \(2017\)](#) inspected the impact of Hall involvement on hydro-magnetic free convection in an upstanding microchannel. To name a few, references like [Chen and Weng \(2005\)](#), [Bunonomo and Manca \(2012\)](#), and [Weng and Chen \(2009\)](#) give more information on this area of study.

Magnetohydrodynamics (MHD) investigations have risen in relevance over the years due to their advantages in several MHD uses, such as MHD generators, cooling baths with cooling metallic plates, electric transformers, and MHD injectors. In chemical and energy technology, the preference of MHD pumps to convey electrically conductive fluids, is already used in some nuclear power plants. Further to these usages, when the fluid is electrically conductive, an imposed magnetic field can substantially encourage buoyancy-induced current ([Jha et al. 2015](#)). In this context, [Ojemeru et al. \(2023\)](#) explored the hydromagnetic flow of an incompressible Casson fluid controlled by radiation in an upright permeable plate. [Obalulu et al. \(2021\)](#) investigated the role of exothermic chemical reactions in the coexistence of variable electric conductivity and magnetic field effects passing between two vertical plates controlled by Arrhenius kinetics. They discovered that varying electric conductivity and concentration buoyancy promote fluid velocity, but activation energy and magnetic field had the opposite effect. [Taid and Ahmed \(2022\)](#) utilized the perturbation series technique to figure out the joint impacts of Soret and heat dissipation on a chemically controlled natural hydromagnetic flow along an angled permeable channel equipped with porous material. [Osman et al. \(2022\)](#) employed the Laplace transformation technique to evaluate the function of hydromagnetic flow on natural convection through an immeasurable inclined channel. [Siva et al. \(2021\)](#) reported on a heat transfer problem of electrokinetic impact in an oscillating microchannel plate and showcased adequate deviations to MHD involvement. [Sandeep and Sugunamma \(2013\)](#) investigated the action of an inclined magnetic field on the transient natural convection of a dusty reactive fluid within two immeasurable plates blended with porous material. References such as [Joseph et al. \(2015\)](#), [Geethan et al. \(2016\)](#), and [Jha et al. \(2023\)](#) further exemplify this phenomenon.

The study of the behaviour of the unique interactions when hydromagnetic natural convection travel in a superhydrophobic surface (SHS) microchannel is gathering much attention from the engineering sciences and technology sectors. Superhydrophobic (SHO) walls have the potential to minimise frictional force in the flow owing to the huge slip caused by liquid/solid relationships,

subsequently making it a helpful condition to measure the extent of drag force due to the slip length ([Jha and Gwandu 2020](#)). The effects of MHD convective flows via a heated SHO microchannel have been studied in a number of systematic build-up works. The theoretical research on MHD-free convection in an upward micro-channel equipped with SHS and temperature jump was carried out by [Jha and Gwandu \(2017\)](#) considering the influence of heating by uniform wall heating while [Jha and Gwandu \(2019\)](#) work; they employed the nonlinear Boussinesq approximation approach to discuss natural convection of an hydromagnetic fluid in a slit micro-channel coated with SHS and temperature jump conditions. Later again, [Jha and Gwandu \(2020\)](#) expanded their earlier work by including the wall porosity effect. Through a heated superhydrophobic microchannel, [Ojemeru and Onwubuya \(2023\)](#) presented their investigation of viscous dissipative fluid in the presence of suction/injection action and mixed convection. The importance of heat radiation and superhydrophobicity on the buoyancy-driven force on a viscous and incompressible fluid over an upright microchannel controlled by an imposed magnetic field was reported by [Hamza et al. \(2023c\)](#). Quite recently, [Yale et al. \(2023\)](#) improved on the research of [Jha and Gwandu \(2017\)](#) by taking into account the impact of viscous dissipative fluid on hydromagnetic natural convection in a heated superhydrophobic microchannel using the regular perturbation technique. In a different study, [Ramanuja et al. \(2020\)](#) assessed free convection in a microchannel that is isothermally heated and has one side having SHS and temperature jump constraints. The implications of heat transport through a cylinder with a non-wetting surface were accurately and explicitly described by [Hatte and Pitchumani \(2021\)](#) using fractional rough wall features. They concluded that, in contrast to the popular assumption, super-hydrophobicity, characterized by the highest contact angles, rarely results in peak convective heat transfer behaviour and that hydrophobic coatings can offer outstanding thermal efficiency under certain fluid flow situations.

Based on the aforementioned literature, there is no previous research on the effects of Arrhenius kinetic on micro-channels with superhydrophobic walls affected by internal heat sources or sinks. Hence, the novelty and the inspiration behind this study. This article aims to, therefore, theoretically evaluate the steady, fully developed free convection of a chemically reacting fluid in an upstanding micro-channel having a superhydrophobic surface driven by heat generation and absorption, thus extending the study done by [Jha and Gwandu \(2017\)](#). The non-dimensional coupled equations are analysed using regular perturbation series. Calculations are also made for physical parameters relevant to engineering, such as the drag force and the heat transfer rate coefficients. The findings of this study could prove highly useful in a variety of fields, including micro-devices manufactured with micro-fabrication methods, micro-electro-mechanical

systems (MEMS), the lubrication industries, biomedical research, the mining industries, and so on.

chemically reactive, heat source/sink driven, and uses the Boussinesq's approximation subject to relevant boundary conditions, have been described as:

**MATERIALS AND METHODS**

**Mathematical Structure of the Flow**

Imagine a steady buoyancy-driven flow of an incompressible, hydromagnetic fluid flowing smoothly upwards over an upward-facing plate microchannel controlled by Arrhenius kinetics and a heat source or sink. One of the sides is exceedingly difficult to wet (superhydrophobic) due to a unique micro-engineering procedure. The other surface was not modified. As shown in Figure 1, the SHS is kept at  $y_0 = 0$ , whereas the no slip side is kept at  $y_0 = L$ . Because a surface's superhydrophilicity is more significant than how it flows, varying heat jumps and slip settings were applied to the different plates. Taking Jha and Gwandu (2017) as a benchmark, the governing equations for the present mathematical model, which assume that the fluid is

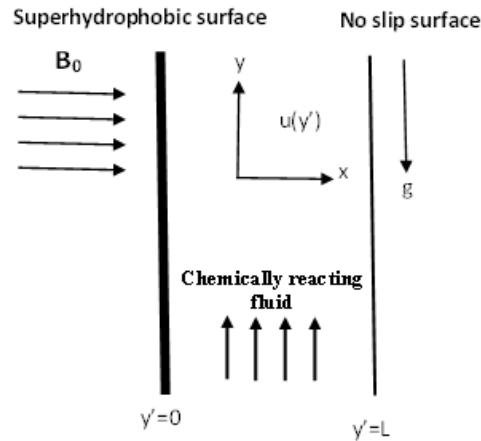


Figure 1 Sketch of the flow configuration

$$\frac{d^2U}{dy^2} + \theta - M^2U = 0 \tag{1}$$

$$\frac{d^2\theta}{dy^2} + \lambda e^{\frac{\theta}{1+\varepsilon\theta}} - Z\theta = 0 \tag{2}$$

Subject to relevant boundary conditions:

$$\theta(y) = 1 + \Gamma \frac{d\theta}{dy}, \quad \text{at } y = 0 \tag{3}$$

$$u(y) = \gamma \frac{du}{dy}, \quad \text{at } y = 0$$

$$\theta(y) = 1 \quad \text{at } y = 1$$

$$u(y) = 0 \quad \text{at } y = 1$$

Where  $\gamma, \Gamma, M, Z, \varepsilon$  and  $\lambda$  are the velocity slip, the temperature jump, the magnetic number, heat source/sink, activation energy, and chemically reacting terms.

The non-dimensional variables applied are:

$$u = \frac{u'}{U}, y = \frac{y'}{h}, T = \frac{T' - T_0}{T_w - T_0}, x = \frac{x'v}{Uh^2}, Z = \frac{Q_0h^2}{k}$$

$$M^2 = \frac{\sigma\beta_0^2h^2}{\rho\nu}, \varepsilon = \frac{RT_0}{E}, \lambda = \frac{QC_0^*AEH^2}{RT_0^2} e^{\left(\frac{-E}{RT_0}\right)}, (Y, \gamma, \Gamma) = (Y', \gamma', \Gamma')/h$$

**Method of Solutions**

The velocity and temperature equations are a set of ordinary differential equations resolved by the regular perturbation approach.

It is assumed that 
$$\left. \begin{aligned} \theta &= \theta_0 + \lambda\theta_1 \\ U &= U_0 + \lambda U_1 \end{aligned} \right\} \tag{4}$$

inserting eqn (4) into eqns (1-3) and comparing the coefficients of  $\lambda^0$  and  $\lambda$ , the sets of equations are derived as:

$$\lambda^0 : \frac{d^2U_0}{dy^2} + \theta_0 - M^2U_0 = 0 \tag{5}$$

$$\lambda : \frac{d^2U_1}{dy^2} + \theta_1 - M^2U_1 = 0 \tag{6}$$

$$\lambda^0 : \frac{d^2\theta_0}{dy^2} - Z\theta_0 = 0 \tag{7}$$

$$\lambda : \frac{d^2\theta_1}{dy^2} - Z\theta_1 = -1 - \theta_0 - (2 - e)\theta_0^2 \tag{8}$$

And the corresponding boundary conditions are:

$$\left. \begin{aligned} U_0 = \lambda \frac{dU_0}{dy} \\ U_1 = \lambda \frac{dU_1}{dy} \\ U_0 = 0 \\ U_1 = 0 \end{aligned} \right\} \begin{array}{l} \text{at } y = 0 \\ \text{at } y = 1 \end{array} \tag{9}$$

and

$$\left. \begin{aligned} \theta_0 = 1 + \gamma \frac{d\theta_0}{dy} \\ \theta_1 = \gamma \frac{d\theta_1}{dy} \\ \theta_0 = 1 \\ \theta_1 = 0 \end{aligned} \right\} \begin{array}{l} \text{at } y = 0 \\ \text{at } y = 1 \end{array} \tag{10}$$

The solutions for temperature and velocity gradients have been determined as follows:

$$\theta_0 = W_1 \cosh(y\sqrt{Z}) + W_2 \sinh(y\sqrt{Z}) \tag{11}$$

$$\begin{aligned} \theta_1 = W_3 \cosh(y\sqrt{Z}) + W_4 \sinh(y\sqrt{Z}) + F_1 + F_2 \cosh(y\sqrt{Z}) + F_3 \sinh(y\sqrt{Z}) \\ + F_4 \cosh^2(y\sqrt{Z}) + F_5 \cosh(y\sqrt{Z}) \sinh(y\sqrt{Z}) + F_6 \sinh^2(y\sqrt{Z}) \end{aligned} \tag{12}$$

$$U_0 = V_1 \cosh(My) + V_2 \sinh(My) \tag{13}$$

$$\begin{aligned} U_1 = V_3 \cosh(My) + V_4 \sinh(My) + E_3 + E_1 \cosh(y\sqrt{Z}) + E_2 \sinh(y\sqrt{Z}) \\ + E_4 \cosh^2(y\sqrt{Z}) + E_5 \cosh(y\sqrt{Z}) \sinh(y\sqrt{Z}) + E_6 \sinh^2(y\sqrt{Z}) \end{aligned} \tag{14}$$

The rate of heat transfer and shear stress coefficients at both surfaces are also computed as:

$$\frac{d\theta}{dy} \Big|_{y=0} = W_2\sqrt{Z} + \lambda[W_2\sqrt{Z} + F_3\sqrt{Z} + F_5\sqrt{Z}] \tag{15}$$

$$\begin{aligned} \frac{d\theta}{dy} \Big|_{y=1} = W_1\sqrt{Z}\sinh(\sqrt{Z}) + W_2\sqrt{Z}\cosh(\sqrt{Z}) + \lambda[W_3\sqrt{Z}\sinh(\sqrt{Z}) + W_4\sqrt{Z}\cosh(\sqrt{Z}) + F_2\sqrt{Z}\sinh(\sqrt{Z}) + \\ F_3\sqrt{Z}\cosh(\sqrt{Z}) + 2\sqrt{Z}F_4\cosh(\sqrt{Z})\sinh(\sqrt{Z}) + F_5\sqrt{Z}(\sinh^2(\sqrt{Z}) + \cosh^2(\sqrt{Z})) + \\ 2\sqrt{Z}F_6\cosh(\sqrt{Z})\sinh(\sqrt{Z})] \end{aligned} \tag{16}$$

$$\frac{dU}{dy} \Big|_{y=0} = V_2M + \lambda[V_4M + E_2\sqrt{Z} + E_5\sqrt{Z}] \tag{17}$$

$$\begin{aligned} \frac{du}{dy} \Big|_{y=1} = & V_1 M \sinh(M) + V_2 M \cosh(M) + \lambda [V_3 M \sinh(M) + V_4 M \cosh(M) + E_1 \sqrt{Z} \sinh(\sqrt{Z}) + \\ & E_2 \sqrt{Z} \cosh(\sqrt{Z}) + 2\sqrt{Z} E_4 \cosh(\sqrt{Z}) \sinh(\sqrt{Z}) + E_5 \sqrt{Z} (\sinh^2(\sqrt{Z}) + \cosh^2(\sqrt{Z})) + \\ & 2\sqrt{Z} E_6 \cosh(\sqrt{Z}) \sinh(\sqrt{Z})] \end{aligned} \quad (18)$$

## DISCUSSION OF THE FINDINGS

The performance evaluation of an Arrhenius kinetic driven by heat-generating and absorbing effects is executed on a steady natural hydromagnetic flow of an electrically conducting fluid travelling across an isothermally heated upward microchannel. One side is equipped with SHS and temperature jump, and the other is unaltered. The steady-state equations are determined using the regular perturbation series approach. Several graphs have been generated to portray the consequences of the main regulating factors, such as the chemically reacting parameter, heat source parameter,  $Z < 0$ , heat sink parameter,  $Z > 0$ , and Hartman number,  $M$ , on fluid velocity and temperature distributions. The default values selected for this analysis are given as ( $\gamma = \Gamma = 1$ ,  $M = 0.5$ ,  $\lambda = 0.001$ ,  $Z = -0.5$ ). It is useful to state that  $Z < 0$  and  $Z > 0$  represent the heat source and heat sink, respectively.

Figures 2a and b indicate how a heat generation or absorption parameter affects the temperature pattern for constant values of  $\gamma = \Gamma = 1$ . Figure 2a shows a rise in temperature for  $Z < 0$ , but Figure 2b exhibits a decrease in temperature for  $Z > 0$ . As a consequence of heat source parameters along the lower plate, higher variations in temperature are expected. This is because after the heat is taken in, the fluid becomes heavier, and the convection flow decreases, contributing to a drop in the temperature of the fluid. On the other hand, a gain in heat output increases the conduction current, making the fluid less heavy and raising its temperature.

Figure 3 depicts the effects of chemical reactions on the fluid temperature. It is conspicuous that, as the value of  $\lambda$  rises, so does the temperature. Hamza (2016) asserted that increasing the amounts of  $\lambda$  significantly strengthens the heating viscosity in the temperature equation and chemical reacting parameters, resulting in a significant temperature increase.

Figures 4a and b explain the actions of elevating the heat source/sink values on the fluid motion distribution. As the heat source ( $Z < 0$ ) and sink ( $Z > 0$ ) are increased, the similar trends exhibited in the temperature profile are replicated in the fluid velocity component. Physically, this is true owing to the additional heat surge, which improves the ability of the system to transport heat. Consequently,

this increases the thermal and fluid movement in the microchannel. Furthermore, it is thought that the heat generation/absorption parameter closest to the plate carries extra heat, making the fluid flow faster and thus increasing the velocity and temperature inside the boundary layer region.

Figure 5 depicts the relationship between  $\lambda$  and fluid velocity. It was clear that as  $\lambda$  grows, so does the fluid mobility. It was also demonstrated that the fluid wall factor reduces as velocity slip increases at the SHO wall. This causes the gas to accelerate, approaching the wall. The noteworthy spike in temperature in response to the higher  $\lambda$  triggers a decrease in fluid viscosity and an ensuing rise in the speed of the fluid motion.

Figure 6 portrays the effect of MHD on the velocity pattern. The trend demonstrates a decreasing influence on velocity (especially maximum velocity) as the strength of the magnetic field escalates (when  $\gamma = \Gamma = 1$ ), which is anticipated due to the presence of Lorentz force acting on the flow pattern.

Figures 7, 8, 9 & 10 show the effect of heat generation and absorption variations on the heat transfer amount, commonly known as the Nusselt number, and skin friction against the chemical reactive parameter. Figures 7a and b illustrate how heat generation affects the heat transfer coefficient. It is important to note that increasing heat generation values accelerate the movement of the fluid at the lower plate, as depicted in Figure 7a, whereas a counter scenario is observed near the wall ( $y = 1$ ), as shown in Figure 7b.

Figures 8a and b indicate the implications of the heat sink on the heat transfer rate. These graphs show that the heat transfer amount increases at the heated wall but lowers it at the cold wall. Figures 9a and b depict the action of heat source on skin friction coefficient. It was noticed that boosting the level of  $Z$  yields a large improvement in the skin friction at the lower superhydrophobic surface, as shown in Figure 9a, while the converse situation happens at the upper plate.

Figures 10a and b show the effect of the heat absorption parameter on shear stress versus the viscous heating term. As illustrated in these plots, raising the heat generation parameter enhances the skin friction at  $y = 0$  but decreases it at  $y = 1$ .

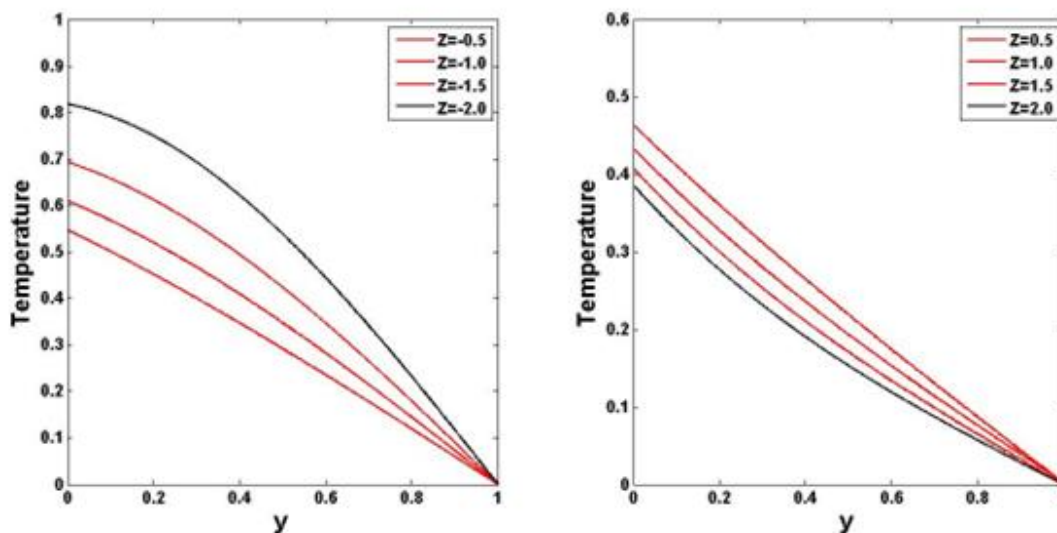


Figure 2: Functions of (a) heat generation and (b) heat absorption on the temperature distributions

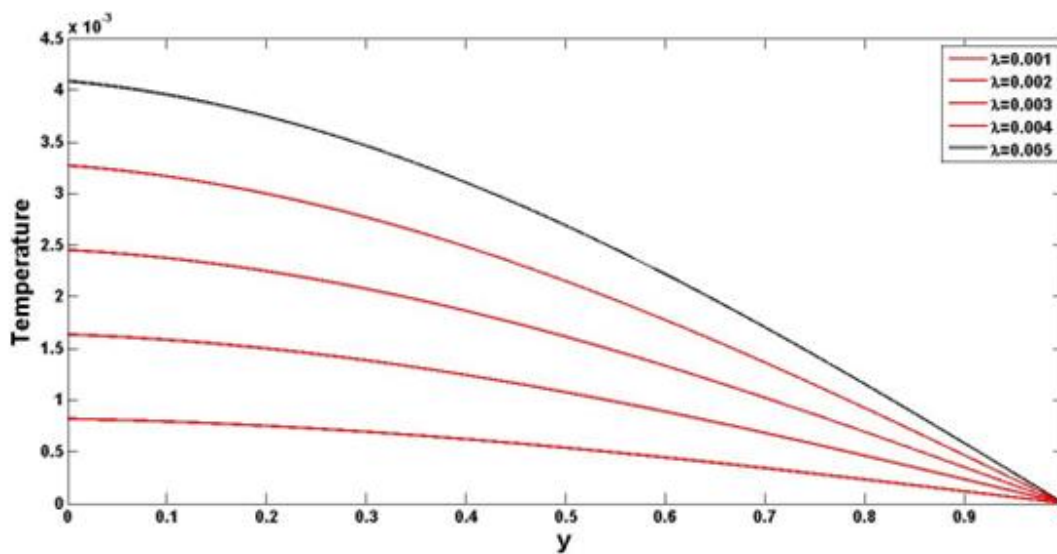


Figure 3: Function of  $\lambda$  on temperature distribution

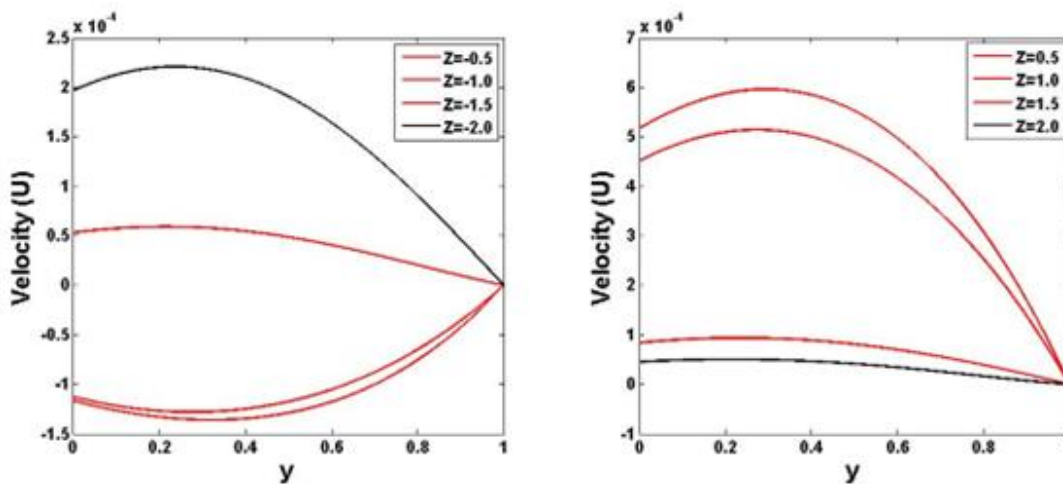


Figure 4: Function of (a) heat generation and (b) heat absorption on velocity distributions

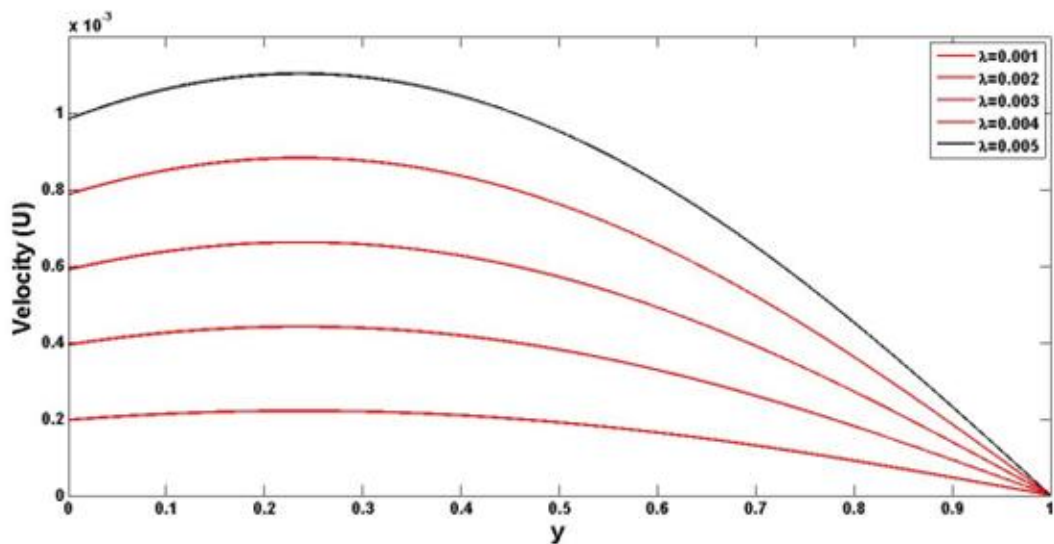


Figure 5: Function of  $\lambda$  on velocity distribution

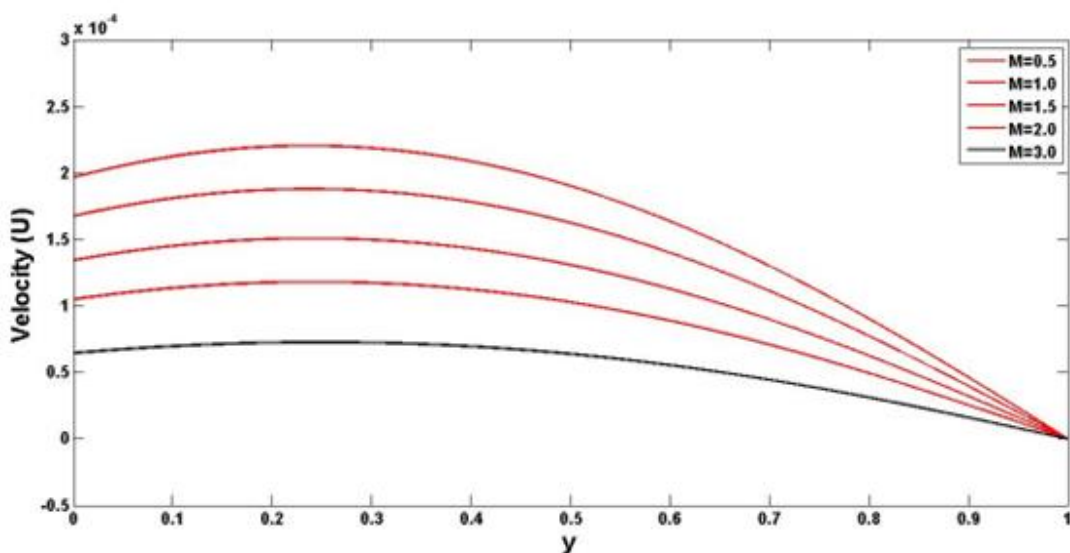


Figure 6: Function of MHD on velocity distribution

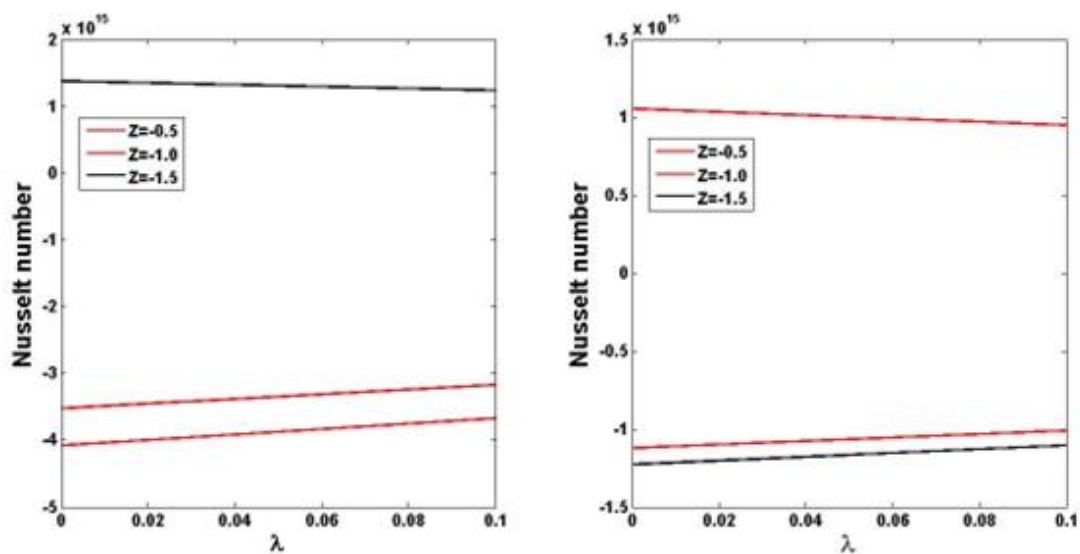


Figure 7: Function of heat generation on Nusselt number at (a)  $y = 0$  and (b)  $y = 1$

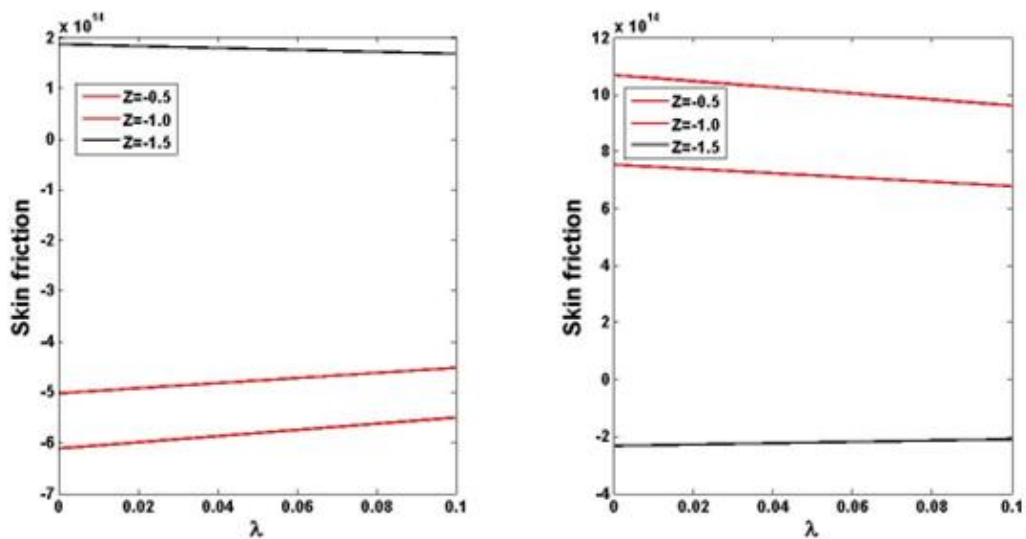


Figure 8: Function of heat absorption on Nusselt number at (a)  $y = 0$  and (b)  $y = 1$

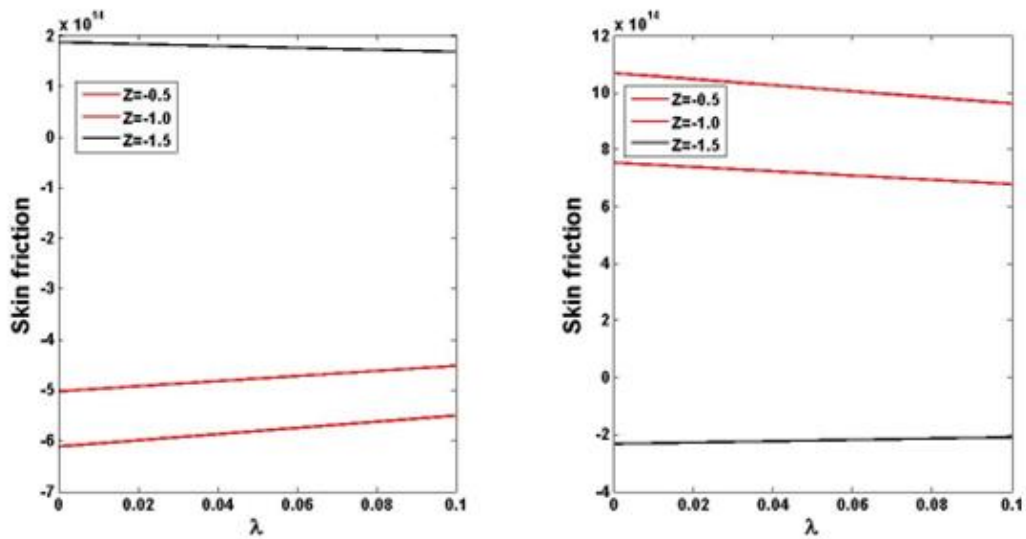


Figure 9: Function of heat generation on skin friction at (a)  $y = 0$  and (b)  $y = 1$

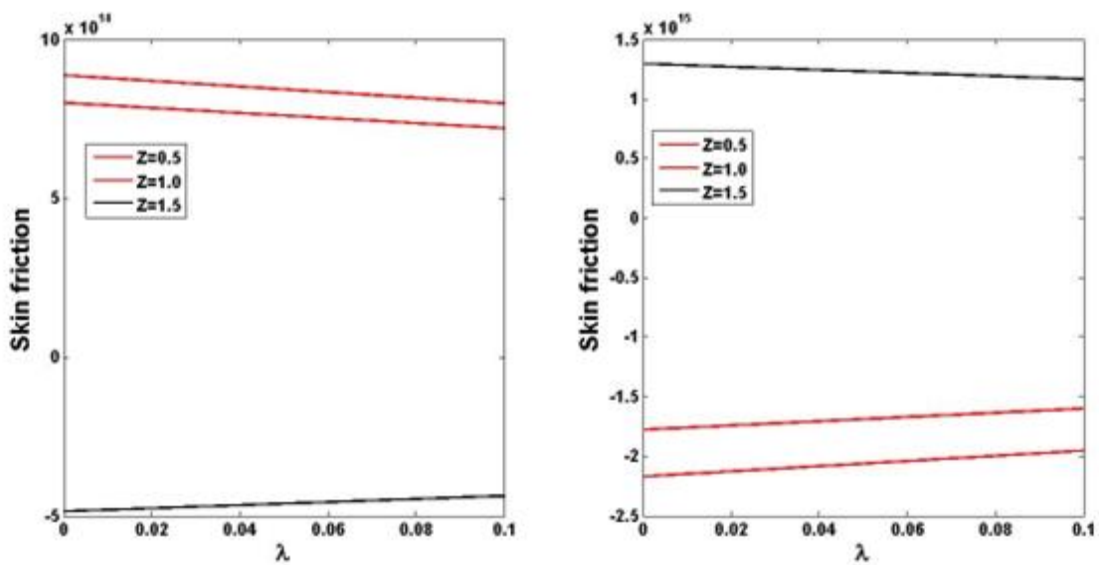


Figure 10: Function of heat absorption on skin friction at (a)  $y = 0$  and (b)  $y = 1$



**RESULTS VALIDATION**

The work of [Jha and Gwandu \(2017\)](#) is retrieved as  $\lambda$  and  $Z$  become zero, respectively, suggesting a strong consistency between the present investigation and their work. The numerical comparison between the work of [Jha and Gwandu \(2017\)](#) with the present study is shown in [Table 1](#).

**Table 1:** Comparison of [Jha and Gwandu's \(2017\)](#) research and the present analysis for velocity and temperature patterns for  $\gamma = \Gamma = 1, M = 0.5$  as  $\lambda$  and  $Z \rightarrow 0$  respectively.

Y	Jha and Gwandu (2017)		Current work	
	$\theta(Y)$	U(Y)	$\theta(Y)$	U(Y)
0.1	0.4500	0.0843	0.4498	0.0843
0.2	0.4000	0.0856	0.4000	0.0856
0.3	0.3500	0.0831	0.3500	0.0831
0.4	0.3000	0.0772	0.2998	0.0772
0.5	0.2500	0.0686	0.2499	0.0686

**CONCLUSION**

The current study discussed the effects of chemically reacting fluids on the steady free convection of an incompressible hydromagnetic fluid moving vertically inside a heated channel plate in the microchannel triggered by heat sink/source, with one side equipped with SHS and temperature jump and the other has no slip. The steady-state system of equations is solved using the regular perturbation series, and various illustrated graphs exhibiting the influence of significant factors on flow characteristics are provided. Understanding these fluids' characteristics is important in engineering and biomedical disciplines. The highlights of the study's principal results are outlined below:

1. The fluid velocity and thermal gradients decrease greatly when  $Z > 0$ , indicating a heat sink. However, when  $Z < 0$ , which represents the heat source, a contrast effect occurs.
2. It was found that a rise in the fluid acceleration and temperature profile is observed as the viscous heating term is intensified.
3. Uplifting the value of  $\lambda$ , the skin friction is lowered at  $y = 0$  but grows at the wall ( $y = 1$ ). Similarly, an identical effect is seen in the heat transfer coefficient for the rising levels of  $\lambda$ .
4. Raising the heat source parameter substantially encourages the drag force and heat transfer rate at the heated wall ( $y = 0$ ), whereas the contrary behaviour is recorded at  $y = 1$ . Also, reverse trends are all demonstrated for growing values of the heat absorption parameter.

**REFERENCES**

Ahmed H., Sadat H. and Nasrazadani S. (2023). High-Fidelity conjugate heat transfer simulation of microchannel heat exchanger, *Fluid Mechanics and Thermal Sciences*, 106(1), pp. 165-181. [[Crossref](#)].

Buonomo, B., and Manca, O., (2012), Natural Convection Flow in a Vertical Micro-Channel with Heated at Uniform Heat Flux, *International Journal of Thermal Science*, 49, pp. 1333-1344. [[Crossref](#)]

Chen. C. K., and Weng, H. C., (2005), Natural convection in a vertical micro-channel, *Journal of Heat Transfer* 127, pp. 1053-1056. [[Crossref](#)]

Geethan, S. K., Kiran, R. K., Vinod, G. K. and Varma, S. V. K., (2016). Soret and Radiation Effects on MHD Free Convection Slip Flow over an Inclined Porous Plate with Heat and Mass Flux, *Advances in Science and Engineering*, 8(3), pp. 1-10. [[Crossref](#)]

Hamza M. M, Ojemer, G. and Ahmad, S. K. (2023). Insights into an analytical simulation of a natural convection flow controlled by Arrhenius kinetics in a micro-channel, *Heliyon* 9(2023) e17628, pp. 1-13. [[Crossref](#)]

Hamza M. M. (2016). Free convection slip flow of an exothermic fluid in a convectively heated vertical channel, *Ain Shams Engineering Journal*, 9(4), pp. 1-11. [[Crossref](#)]

Hamza, M. M. Ojemer, G. and Ahmad, S. K. (2023). Theoretical study of Arrhenius-controlled heat transfer flow on natural convection affected by an induced magnetic field in a microchannel, *Engineering Reports*, [[Crossref](#)]

Hamza, M. M., Bello, I., Mustapha, A., Usman, U. and Ojemer, G. (2023). Determining the role of thermal radiation on hydro-magnetic flow in a vertical porous superhydrophobic microchannel, *Dutse Journal of Pure and Applied Sciences*, 9(2b), pp. 297-308. [[Crossref](#)]

Hatte, S. and Pitchumani, R. (2021). Analysis of convection heat transfer on multiscale rough super-hydrophobic and liquid infused surfaces, *Chemical Engineering Journal*, 424, pp. 1-29. [[Crossref](#)]

Jha, B. K, Altine, M. M. and Hussaini, A. M. (2023). MHD steady natural convection in a vertical porous channel in the presence of point/line heat source/sink: An exact solution, *Heat Transfer*, Wiley, pp. 1-15. [[Crossref](#)]

Jha, B. K. and Aina, B., Isa, S. (2015). Fully developed MHD natural convection flow in a vertical annular micro channel: an exact solution, *Journal*

- of king Saudi University for Sciences, 27, pp. 253-259. [[Crossref](#)]
- Jha, B. K. and Gwandu, B. J. (2019). MHD free convection flow in a vertical slit micro-channel with super-hydrophobic slip and temperature jump: non-linear Boussinesq approximation approach, SN Applied Sciences, 1, 603. [[Crossref](#)]
- Jha, B. K. and Gwandu, B. J. (2020). MHD free convection flow in a vertical porous super-hydrophobic microchannel, Proceedings of the Institution of Mechanical engineers; Part E: Journal of Process of Mechanical Engineering, 235(2), pp. 1-13. [[Crossref](#)]
- Jha, B. K., Aina, B. and Joseph, S. B. (2014b), Natural Convection Flow in vertical Micro-channel with Suction/Injection, Journal of Proceedings of Mechanical Engineering, 228(3), pp. 171-180. [[Crossref](#)]
- Jha, B. K., Aina, B., and Ajiya, A. T., (2014a). MHD natural convection flow in a vertical parallel plate microchannel, Ain shams Engineering Journal, 6, pp. 289-295. [[Crossref](#)]
- Jha, B. K., and Gwandu, B. J., (2017). MHD free convection flow in a vertical slit micro-channel with super-hydrophobic slip and temperature jump: Heating by constant wall temperature, Alexandria Engineering Journal, 57(3), pp. 2541-2549. [[Crossref](#)]
- Jha, B. K., and Malgwi, P. B., (2019a). Hall current and ion – slip effects on free convection flow in a vertical microchannel with induced magnetic field, Heat Transfer Asian Research 48(8), pp. 1 – 19. [[Crossref](#)]
- Jha, B. K., Malgwi, P. B. and Aina, B. (2017). Hall effects on MHD natural convection flow in a vertical micro-channel. Alexandria Engineering Journal, [[Crossref](#)]
- Joseph, K. M., Ayuba, P., Nyitor, L. N. and Muhammed, S. M. (2015). Effect of Heat and Mass Transfer on Unsteady MHD Poiseuille flow between Two Infinite Parallel Porous plates in an Inclined Magnetic Field, International Journal of Scientific Engineering and Applied Science, 1(5).
- Obalalu, A. M., O. A. Ajala, A. T. Adeosun, A. O. Akindele, O. A. Oladapo and O. A. Olajide, (2021). Significance of variable electrical conductivity on non-Newtonian fluid flow between two vertical plates in the coexistence of Arrhenius energy and exothermic chemical reaction, Partial Differential Equation in Applied Mathematics, 4, 100184, pp. 1-9. [[Crossref](#)]
- Ojmeri, G. and Hamza, M. M., (2022). Heat transfer analysis of Arrhenius-controlled free convective hydromagnetic flow with heat generation/absorption effect in a micro-channel, Alexandria Engineering Journal, 61, pp. 12797-12811. [[Crossref](#)]
- Ojmeri, G. and Onwubuya, I. O. (2023). Exploring the dynamics of viscous dissipative fluid past a super-hydrophobic microchannel in the coexistence of mixed convection and porous medium, Saudi Journal of Engineering Technology, 8, pp.71-80. [[Crossref](#)]
- Ojmeri, G., Omokhuale, E., Hamza, M. M., Onwubuya, I. O. and Shuaibu, A. (2023). A Computational Analysis on Steady MHD Casson Fluid Flow Across a Vertical Porous Channel Affected by Thermal Radiation Effect. International Journal of Science for Global Sustainability, 9(1), [[Crossref](#)]
- Osman, H. I., Omar, N. F. M., Vieru, D. and Ismail, Z. (2022). A study of MHD free convection flow past an infinite inclined plate, Journal of Advanced Research in fluid Mechanics and Thermal Sciences, 92(1), pp. 18-27. [[Crossref](#)]
- Ramanuja, M., Krishna, G. G., Sree, H. K. and Radhika, V. N. (2020). Free convection in a vertical slit microchannel with super-hydrophobic slip and temperature jump conditions, International Journal of Heat Technology, 38(3), pp. 738-744. [[Crossref](#)]<https://doi.org/10.18280/ijht.380318>
- Sandeep, N. and Sugunamma, V. (2013). Effect of an Inclined Magnetic Field on Unsteady free Convection flow of a Dusty Viscous fluid between two Infinite flat Plates filled by a Porous medium, International Journal of Applied Mathematics and Modeling, 1(1), pp. 16-33.
- Siva, T., Jaangili, S. and Kumbhakar, B. (2021). Heat transfer analysis of MHD and electroosmotic flow of non-Newtonian fluid in a rotating microfluidic channel: an exact solution, Applied Mathematics and Mechanics, 42, pp. 1047-1062. [[Crossref](#)]
- Taid, B. K., and Ahmed, N. B., (2022), MHD free convection flow across an inclined porous plate in the presence of heat source, solet effect and chemical reaction affected by viscous dissipation ohmic heating, Bio-interface Research in Applied Chemistry 12(5) pp. 6280-6296. [[Crossref](#)]
- Weng, H. C. and Chen, C. K., (2009), Drag reduction and heat transfer enhancement over a heated wall of a vertical annular microchannel, International Journal of Heat and Mass Transfer, 52, pp. 1075–1079. [[Crossref](#)]

**APPENDICES**

$$F_1 = \frac{1}{Z}, F_2 = \frac{-W_1}{Z^2 - Z}, F_3 = \frac{-W_2}{Z^2 - Z}, F_4 = \frac{-n_1 W_2^2 - F_6(2Z^2 - Z)}{2Z^2}, F_5 = \frac{-2n_1 W_1 W_2}{4Z^2 - Z},$$

$$F_6 = \frac{-2n_1 Z^2 W_1^2 + n_1 W_2^2(2Z^2 - Z)}{4Z^4 - (2Z^2 - Z)^2}$$

$$n_1 = 2 - e, n_2 = F_1 + F_2 + F_4, n_3 = \sqrt{Z}(F_3 + F_5), n_4 = \Gamma n_3 - n_2, n_5 = F_1 + F_2 \cosh(\sqrt{Z}) + F_3 \sinh(\sqrt{Z}) + F_4 \cosh^2(\sqrt{Z}) + F_5 \cosh(\sqrt{Z}) \sinh(\sqrt{Z}) + F_6 \sinh^2(\sqrt{Z}), W_2 = \frac{-\cosh(\sqrt{Z})}{\Gamma \sqrt{Z} \cosh(\sqrt{Z}) + \sinh(\sqrt{Z})},$$

$$W_1 = 1 + \Gamma W_2 \sqrt{Z}, W_3 = \Gamma W_4 \sqrt{Z} + \Gamma n_3 - n_2, W_4 = n_7 / n_6,$$

$$E_1 = \frac{-(W_3 + F_2)}{Z^2 - M^2}, E_2 = \frac{-(W_4 + F_3)}{Z^2 - M^2}, E_3 = \frac{F_1}{M^2}, E_4 = \frac{-F_4(2Z^2 - M^2) + 2Z^2 F_6}{(2Z^2 - M^2) - 4Z^2}, E_5 = \frac{F_5}{4Z^2 - M^2}$$

$$E_6 = \frac{-F_4(2Z^2 - M^2) + 2Z^2 F_6}{(2Z^2 - M^2)^2 - 4Z^4}, n_8 = E_1 \cosh(\sqrt{Z}) + E_2 \sinh(\sqrt{Z}) + E_3 + E_4 \cosh^2(\sqrt{Z})$$

$$+ E_5 \cosh(\sqrt{Z}) \sinh(\sqrt{Z}) + E_6 \sinh^2(\sqrt{Z}), n_9 = \gamma M \cosh(M) + \sinh(M),$$

$$n_{10} = n_9 \cosh(M) - \gamma \sqrt{Z}(E_2 + E_5) \cosh(M) - n_8, V_3 = \gamma(V_4 M + \sqrt{Z}(E_2 + E_5)) - E_1 - E_3 - E_4, V_4 = \frac{n_{10}}{n_9}$$